Published in final edited form as:
*Integr Biol (Camb)*. 2012 March ; 4(3): 328–334. doi:10.1039/c2ib00083k.

# Cell cycle synchronization by nutrient modulation†

**Yuan Tian**[a,b], **Chunxiong Luo**[a,b], **Yuheng Lu**[c], **Chao Tang**[b,d], and **Qi Ouyang**[a,b]

Chunxiong Luo: pkuluocx@pku.edu.cn; Qi Ouyang: qi@pku.edu.cn

[a]Center for Microfluidic and Nanotechnology, The State Key Laboratory for Artificial Microstructures and Mesoscopic Physics, School of Physics, Peking University, Beijing, 100871, China; Tel: +86-10-62751425, +86-10-62756943

[b]Center for Theoretical Biology, Academy for Advanced Interdisciplinary Studies, Peking University, Beijing, 100871, China

[c]College of Life Sciences, Peking University, Beijing, 100871, China

[d]Department of Bioengineering and Therapeutic Sciences, University of California, San Francisco, CA 94158, USA

## Abstract

Living cells respond to changing environments by regulating their genes and activities. In unicellular organisms such as yeasts, the cell division cycle is coupled to the nutrient availability. However, it is unclear how tight this coupling is and how the intrinsic time scales of the different cell cycle processes respond to varying nutrient conditions. Here we study the cell cycle behavior of the budding yeast *Saccharomyces cerevisiae* in response to periodically modulated nutrient availability, using a microfluidic platform which allows for longtime cultivation, programmed medium switching, and automated time-lapse image acquisition. We observe that the division cycle of the yeast cells can follow a periodically modulated medium so that the whole population can be driven into synchrony. When the period of the nutrient modulation is optimized, as many as 80% of the cells in a population are continuously synchronized. The degree of synchronization as a function of the nutrient modulation period can be qualitatively captured by a stochastic phenomenological model. Our work may shed light on the coupling between the cell growth and cell division as well as provide a nontoxic and non-invasive method to continuously synchronize the cell cycle.

## Introduction

A hallmark of the living systems is their ability to adapt to the changing environment. At the physiological time scales and at the cellular level, the adaptation is achieved by regulating the activities of genes and proteins. How cells implement such a regulation is a central question in biology. A prototypical example is how cells regulate their division cycle in response to nutrient availability, which limits the rate at which they can grow. Recent advances in microfluidics technology[1–4] made it possible to precisely control the cellular environment at the single cell level. In this paper, we apply the technology to address questions concerning the coupling between the nutrient conditions and the cell division cycle in the unicellular organism *Saccharomyces cerevisiae* (budding yeast). Specifically, we investigate the yeast cell cycle behavior in response to periodically varied nutrient conditions.

†Electronic supplementary information (ESI) available. See DOI: 10.1039/c2ib00083k

Correspondence to: Chunxiong Luo, pkuluocx@pku.edu.cn; Qi Ouyang, qi@pku.edu.cn.

From a nonlinear dynamics point of view, the recurrent cell cycle progression may be considered as a certain kind of biochemical oscillation. As a result if an external stimulation has unequal effects on different cell cycle phases—*e.g.* accelerating or decelerating a particular phase—a periodic repetition of this stimulation can be exploited to produce "phase-locking"[5] in the cell cycle control systems. In budding yeast, the $G_1$ phase is most sensitive to nutrient conditions in the sense that the prolonged cell cycle period in poor nutrients can be mostly accounted for by a prolonged $G_1$ phase.[6–11] This information leads to our idea that cells can be synchronized by oscillating rich and poor nutrients at the correct period, amplitude and durations of each phase. Whether, under what conditions, and with what fraction of the cells in the population such a synchronous behavior will happen are the questions we address in this work. Answers to these questions may help us to better understand the coupling between cell growth and cell division.

From a practical point of view, our study provides a useful way to synchronize the cell cycle in a cell population. Considerable efforts have been made to develop cell cycle synchronization methods and technologies,[12–15] which are of critical importance in molecular biology, genetic and genomic studies.[16–18] Most of these methods involve biochemical reagents that block cell cycle progression, thus disrupting cellular functions and potentially introducing toxicity.[19,20] Nontoxic sorting of cells of different phases, such as with FACS, is unsuitable for cells without particular fluorescent signals or size characteristics. Less invasive methods to synchronize the cell cycle, usually involving nutrient depletion, such as arresting the cells at the $G_0$ phase by incubating yeast with no glucose medium or growing bacteria to the "stationary phase" to enrich cells uncommitted to division, were also developed.[21,22] However, these methods are time-consuming,[21] cumbersome to operate, and have difficulty in sustaining a continuous (through many cycles) high-level synchrony. The use of a microfluidic device to synchronize the cell cycle in a non-invasive, continuous and automated fashion may open the door for many applications.

## Experimental setup

To monitor the long-time behavior of cell population under periodic nutrient modulation, we developed a cultivation-observation device. This device consists of a microfluidic chip as the cultivation module, a group of computer controlled syringe pumps as the feeding module, and a Nikon Ti microscope equipped with a programmable motorized stage and a CCD camera as the data acquisition module (Fig. 1A). Using the standard soft-lithography method, four equivalent modules with dozens of square shaped growth chambers were fabricated in every PDMS microfluidic chip (ESI†, Fig. S1). The height of the growth chambers (3.5 μm) was a little less than the yeast cell diameter, so that the expanding yeast colonies in the chambers will be constrained in the monolayer (Fig. 1B). A markedly higher feeding channel (200 μm wide, 10 μm high and about 20 mm long) was fabricated to connect these chambers (with necks of 40 μm wide and 3.5 μm high), and two syringe pumps dispensed rich/poor culture medium through this channel, respectively, the dispensation procedure was automated using a custom MATLAB program. Nutrient and waste exchange between the feeding channel and the growth chambers is mainly through diffusion. The linear size of the cultivation chamber is 120 μm, the diffusion time is about 1 min. Two pumps pushed alternately rich and poor culture medium into the feeding cannel, in this case the nutrient concentration in the culture environment can be considered as a square-wave function of time with a time resolution of 1 min. During the whole process, little cell movement or shear stress was introduced.[23] The images of the growing yeast colonies were acquired under the control of *NIS-Elements AR* software (Nikon, version 3.10). Employing

†Electronic supplementary information (ESI) available. See DOI: 10.1039/c2ib00083k

a motorized *x*–*y* stage and a PFS (perfect focus system) focus maintain unit, the microscope scans a series of points of interest every 5 minutes.

To mark the cell cycle phase of the budding yeast, we used an MCM marker fused with an mCherry fluorescent protein. The MCM marker is localized in the nucleus during the $G_1$ phase, and is exported from the nucleus during the S and M phases[24] (Fig. 1C). In the experiments the bright field and fluorescence micrographs of the colonies in the microfluidic chip were acquired at a 5-minute interval. Using semi-automatic software the $G_1$ and non-$G_1$ cells in every image were recognized. Position difference of the same cell in two successive frames is tiny, so that the cell moving trajectories and the cell lineage relationship can be traced out, and the phase transition times of every cell can be determined. In the study we used the $G_1$ index (the fraction of the $G_1$ cells in the colony) to quantify the degree of synchronization in budding yeast colonies.

## Experimental observations

Fig. 2 illustrates the mechanism of cell cycle synchronization using alternating rich and poor media. Initially, in a yeast population growing in rich medium (see Methods), cells distribute evenly throughout the cell cycle phases. When treated with poor medium (see Methods), the $G_1$ phase is prolonged and cells in $G_1$ tend to stay in $G_1$, but non-$G_1$ cells continue to progress through the S and M phases to enter the $G_1$ phase, so that the fraction of $G_1$ cells in the population increases. When the medium is switched back to rich medium, the accumulated $G_1$ cells rapidly progress out of the $G_1$ phase, resulting in a large percentage of the cells in a similar phase. If the switching between rich and poor media is applied repeatedly with suitable periods, the degree of cell cycle synchronization may be enhanced.

Note that for the budding yeast the degree of synchronization is intrinsically constrained by the asymmetrical division of the cell, which results in a smaller daughter cell compared with the mother. Consequently, the daughter cell will have a longer $G_1$ phase in order to grow bigger. Another two major sources for de-synchronization are noise and cell variability.[25] Nonetheless, we found that a high degree of synchronization can be achieved with a well-designed combination of poor and rich medium periods and compositions.

With the microfluidic device described above we carried out a series of experiments with various modulation schemes. Fig. 3A shows the pedigree tree of a typical colony modulated by a scheme of 60 min period of poor medium alternating with 90 min period of rich medium. $G_1$ and non-$G_1$ phases are indicated with red and green colors, respectively. One observes that the cell cycle phases in one colony get more and more synchronized with the media modulation; they reach the maximum degree of synchronization after three poor-rich media switching periods. Notice that at the beginning of the modulation the doubling times for mother and daughter cells are very different, but they become similar after three modulation periods. When the periodic modulation is switched to a continual rich medium, the cell population quickly de-synchronized and the cell cycle phase distribution became flat (see right-most part of Fig. 3). Fig. 3B shows the $G_1$ index of four colonies in different growth chambers but under the same nutrient modulation scheme. The data indicate that initial populations with obvious cell cycle phase differences can be effectively synchronized into the same phase state. As many as 80% of the cells in a population can be synchronized.

We also performed experiments with different periodic modulation schemes and found that most of them can induce cell cycle synchronization, but with different degrees. Fig. 4A–G show the $G_1$ index under different media modulation schemes (more data in Fig. S2, ESI†). From these data one observes that all modulation schemes can drive the $G_1$ index into oscillation to some extent, but only the 75p + 75r and 60p + 90r schemes can realize a maximum oscillation amplitude (from 20% to 80%). When the modulation scheme departs

from these two schemes, the amplitude of $G_1$ index oscillation drops, indicating the decline of the synchronization degree. In each of the modulation schemes shown in Fig. 4, the periodic modulation of poor and rich media is repeated 5 times and then the medium is left rich. One observes that the $G_1$ index continued to oscillate, but the amplitude diminished dramatically. The population quickly de-synchronizes without a periodic medium modulation. For a population incubated with a constant rich medium, the $G_1$ index varied little throughout the expansion of the population (ESI†, Fig. S2H).

## Synchronization mechanism and model

This method is based on the fact that the length of the $G_1$ phase of budding yeast is more sensitive to starvation. Many key steps in the budding yeast cell cycle have been reported in the literature. In the $G_1$ phase cells need to produce some regulatory protein such as Cln3, whose abundance is governed by the availability of nutrient. By phosphorylating Whi5 and then activating SBF/MBF, Cln3 promotes the transition to the S phase. So the key step in the $G_1$ phase may be the accumulation of regulatory proteins. Starvation will slow down these courses. The key steps in the non-$G_1$ phase should be the cell division process such as DNA replication, spindle pole body duplication, spindle assembly, chromatin segregation *etc.*, which have little connection to extracellular nutrition.

To account for the observed synchronization of the cell cycle phases under the poor-rich medium modulation, we first measured the distribution of the length (time duration) of $G_1$ and non-$G_1$ phases for populations in rich and poor media, and for mother and daughter cells, respectively (Fig. 5, vertical bars, and Table S1, ESI†). From these data, we observe that (1) in all cases there is a significant variability in the length of the cell cycle phase;[26] (2) both the $G_1$ and non-$G_1$ lengths are prolonged in poor medium compared with those in rich medium, but the $G_1$ phase lengths are prolonged more significantly; (3) mother and daughter cells have distinct length distributions in $G_1$, and both vary under the nutrient conditions (Fig. 5A–D); (4) mother and daughter cells have very similar length distribution for non-$G_1$ phase (ESI†), which only changes under the nutrient conditions (Table S1, ESI†). These observations led us to construct the following phenomenological stochastic model.

In the model the cell cycle process is considered as a series of ordered events or steps. The progression of the cell cycle is then successive transitions from one step to the next. The parameters of the model are the number of steps and the transition probability. Specifically, a phase ($G_1$/non-$G_1$) of a cell (mother/daughter) cultivated in a growth medium (rich/poor) was divided into $k$ hypothetical steps, and cell cycle progression was interpreted as a "leap forward" event along these steps irreversibly. At every time step of evolution, a cell had a chance $p$ to jump from the current step to the next on the events chain. In this model, the duration $j$ (in terms of the time steps) of a cell cycle phase satisfies the negative binomial distribution (the probability that the cell traveled through a cell cycle phase in $j$ simulation steps):

$$N(j)=C_{j-1}^{k-1}p^k(1-p)^{j-k}.$$

To derive the parameters $k$ and $p$ for different cases (mother/daughter cell, rich/poor medium, $G_1$/non-$G_1$ phase), we fitted the negative binomial distribution to the measured phase length distribution data. Given the similarity of phase length distributions for daughter and mother cells in the non-$G_1$ phase, six sets of parameters were obtained (Table S2, ESI†). In this model, $k/p$ is the expected simulation steps of a phase, $k(1-p)/p^2$ is the variance, $t_0k/p$ is the expected duration of the phase (here one simulation step represents $t_0$ of time). With the same expected duration, the smaller the $k$ is, the larger the fluctuation of a phase is. Both

the expected value and the variance of duration are important for the phenomena, the parameters (*k, p*) determine these two most important features of negative binomial distribution. The fitted distribution is compared with the experimental data in Fig. 5. One observes that the phase length distribution for all cases agrees well with the negative binomial distribution.

By performing simulations using the obtained parameters (see ESI† for details), we qualitatively reproduced the modulation effect of different schemes: the strongest synchronization is achieved by modulation schemes with a period of around 150 min; elongating or shortening the modulation period will decrease the degree of synchronization. The simulation results corresponding to three typical modulation schemes are plotted in Fig. 6.

## Discussion

We have studied the cell cycle phases of budding yeast populations under periodically modulated nutrient supply using a microfluidic device. We observed continuously synchronous populations in a range of modulation schemes. When the nutrient modulation scheme is optimized, more than 80% cells in the population can be synchronized. To account for our experimental observations we have constructed a mathematical model, which agrees well with the experiments. At present the molecular mechanisms for the coupling among the nutrient conditions, cell growth, and cell division are far from being clear,[10,27] and “size control” is by now the most widely accepted concept to explain the coordination of cell growth and division. But in this work, we start our idea from the fact that the $G_1$ phase of the budding yeast cell cycle is especially sensitive to starvation, this leads us to build a phenomenological model, which involves no molecular details but the simple assumption that the cell cycle progresses as irreversible stochastic transitions in successive steps. The absence of molecular details in our model limited its possibilities for providing more biological insights into gene networks, but the abstract features of this model give it an advantage for ease application in predicting the most effective modulation schemes, especially in the context that an organism needs to be synchronized but the molecular details of its cell cycle control network are poorly understood.

Our work adds new dimensions and tools in the study of the coupling between cell growth and cell division. The precise temporal control of the cellular environment together with the automated image acquisition and analysis provides an efficient way to quantitatively probe the system. Further questions concerning the cells’ behavior in response to fluctuating environments can be addressed, some of which are already underway in our lab.

Prior to this work there have been many approaches that were developed to synchronize the cell cycle in biological studies. One of the most significant advantages of our method is that neither chemical inhibitors of cellular processes are introduced, nor genetic modification is involved, so there are no potential toxic effects on the cell, and the normal cellular functions will not be disrupted. Some earlier studies produced synchronization in budding yeast colonies by periodical induction of cyclin expression, their artificial gene modifications were necessary.[4,28] In contrast, our synchronization method can be used in most strains without any genetic modifications, and a short period of nutrient depletion causes little interference to cell. The second advantage is that the method is easy to use. Conventional nontoxic synchronization methods such as centrifugal elutriation and fluorescence activated cell sorting require expensive equipments and they can be tedious to synchronize the population continuously. It is also difficult to combine those conventional methods with high-resolution dynamic measurements as can be done in the microfluidic device. The third advantage is that the principle adopted here is generally applicable to many different

organisms, from prokaryotic bacteria[22] to mammalian cells, as nutrients and/or growth factors can modulate the cell growth and division for a wide variety of cells. To demonstrate the generality of our synchronization method, the similar modulation schemes were also applied to fission yeast (*Schizosaccharomyces pombe*). We found that appropriate modulation periods can efficiently synchronize the cell cycle in a population (Fig. S3, ESI†).

The cell cycle process is often considered as an example of biochemical oscillation. Although in some cases, *e.g.* in *Xenopus* eggs, there is clearly an autonomous oscillator underplay,[29] it is unclear that in the budding yeast the process is controlled by an autonomous oscillator or if there are multiple recurrent processes (which may include certain kinds of oscillators) coupled together.[30–32] From a nonlinear dynamics point of view, an autonomous oscillator can "phase-lock" to an external periodic stimulus when the stimulus period is close to the intrinsic period of the oscillator.[5] This phenomenon has been investigated in budding yeast, using an artificially constructed strain, in which an exogenous $G_1$ cyclin gene is induced periodically to trigger the cell cycle.[4] However, because nutrient depletion delays the progression of the cell cycle, the intrinsic period of the cell cycle varies with different modulation situation. In our experiments, we find that the best "locking" (the largest faction of synchronous cells in a population) happens at a longer modulation period (150 min) than the natural cell cycle period (about 100 min) of continual rich media.

## Methods

### Yeast strain, media and cell preparation

The *Saccharomyces cerevisiae* strain used in this experiment is YCT50 (MAT a his3Δ met3Δ ura3Δ leu2Δ ura MYO1::MYO1-GFP::HIS3[pGREG506 ADH1pr-MCM-mCherry]). Before each experiment a single colony was inoculated in culture medium SC $His^-$ $Ura^-$, shaken at 30 °C over night, diluted to about $10^6$ cells per ml with the medium, and grown to about $10^7$ cells per ml. The rich medium used in budding yeast modulation experiments was SC $His^-$ $Ura^-$, the poor medium was a mixture of 1.5% SC $His^-$ $Ura^-$ and 98.5% PBS (phosphate-buffered saline, pH = 6.0). In preliminary experiments we recognized that only when the percentage of SC $His^-$ $Ura^-$ was reduced to below 4% the cell cycle progression can be affected effectively. The temperature of the chip, medium and microscope lens was maintained at 30 °C in yeast experiments.

### Micrograph analysis

We used custom semi-automatic software developed in C# with Microsoft Visual Studio 2010 Express Edition for micrograph analysis. Every cell in a colony was traced from the last micrograph frame to the frame where it was born, the cell cycle phase transition, moving trajectory and lineage relationship were recorded, the $G_1$ index and the pedigree tree were plotted and the cell cycle phase durations were calculated.

## Acknowledgments

The authors would like to thank X. L. Liu, X. J. Yang, L. L. Jiang, X. J. Zhu and G. W. Si for helpful discussions. This work is partially supported by the NSF of China (11021463, 11074009, 10704002, 11174012), the MOST of China (2009CB918500), the NFFTBS of China (J0630311). C. T. acknowledges support from NSF and NIH (P50 GM081879).

## References

1. Shimizu TS, Tu Y, Berg HC. Mol Syst Biol. 2010; 6:382. [PubMed: 20571531]
2. Kalinin YV, Jiang L, Tu Y, Wu M. Biophys J. 2009; 96:2439–2448. [PubMed: 19289068]

3. Keymer JE, Galajda P, Muldoon C, Park S, Austin RH. Proc Natl Acad Sci U S A. 2006; 103:17290–17295. [PubMed: 17090676]
4. Charvin G, Cross FR, Siggia ED. Proc Natl Acad Sci U S A. 2009; 106:6632–6637. [PubMed: 19346485]
5. Strogatz, SH. Nonlinear dynamics and Chaos: with applications to physics, biology, chemistry, and engineering. Addison-Wesley Pub; Reading, Mass: 1994.
6. Temin HM. J Cell Physiol. 1971; 78:161–170. [PubMed: 5167847]
7. Pardee AB. Proc Natl Acad Sci U S A. 1974; 71:1286–1290. [PubMed: 4524638]
8. Prescott DM. Adv Genet. 1976; 18:99–177. [PubMed: 181964]
9. Brauer MJ, Huttenhower C, Airoldi EM, Rosenstein R, Matese JC, Gresham D, Boer VM, Troyanskaya OG, Botstein D. Mol Biol Cell. 2008; 19:352–367. [PubMed: 17959824]
10. Jorgensen P, Tyers M. Curr Biol. 2004; 14:R1014–R1027. [PubMed: 15589139]
11. Unger MW, Hartwell LH. Proc Natl Acad Sci U S A. 1976; 73:1664–1668. [PubMed: 775494]
12. Keyomarsi K, Sandoval L, Band V, Pardee AB. Cancer Res. 1991; 51:3602–3609. [PubMed: 1711413]
13. Hartwell LH. Bacteriol Rev. 1974; 38:164–198. [PubMed: 4599449]
14. Prescott, DM. Methods in cell physiology. Academic Press; New York, London: 1970.
15. Mitchison JM, Creanor J. Exp Cell Res. 1971; 67:368–374. [PubMed: 4255493]
16. Spellman PT, Sherlock G, Zhang MQ, Iyer VR, Anders K, Eisen MB, Brown PO, Botstein D, Futcher B. Mol Biol Cell. 1998; 9:3273–3297. [PubMed: 9843569]
17. Whitfield ML, Sherlock G, Saldanha AJ, Murray JI, Ball CA, Alexander KE, Matese JC, Perou CM, Hurt MM, Brown PO, Botstein D. Mol Biol Cell. 2002; 13:1977–2000. [PubMed: 12058064]
18. Whitfield ML, Zheng LX, Baldwin A, Ohta T, Hurt MM, Marzluff WF. Mol Cell Biol. 2000; 20:4188–4198. [PubMed: 10825184]
19. Samake S, Smith LC. J Exp Zool. 1996; 274:111–120. [PubMed: 8742691]
20. Generoso WM, Katoh M, Cain KT, Hughes LA, Foxworth LB, Mitchell TJ, Bishop JB. Mutat Res Fundam Mol Mech Mutagen. 1989; 210:313–322.
21. Williamson DH, Scopes AW. Nature. 1962; 193:256–257.
22. Cutler RG, Evans JE. J Bacteriol. 1966; 91:469–476. [PubMed: 5327475]
23. Luo C, Jiang L, Liang S, Ouyang Q, Ji H, Chen Y. Biomed Microdevices. 2009; 11:981–986.
24. Liku ME, Nguyen VQ, Rosales AW, Irie K, Li JJ. Mol Biol Cell. 2005; 16:5026–5039. [PubMed: 16093348]
25. Raser JM, O'Shea EK. Science. 2004; 304:1811–1814. [PubMed: 15166317]
26. Di Talia S, Skotheim JM, Bean JM, Siggia ED, Cross FR. Nature. 2007; 448:947–951. [PubMed: 17713537]
27. Morgan, DO. The Cell Cycle Principles of Control. New Science Press; London, UK: 2007.
28. Charvin G, Cross FR, Siggia ED. PLoS One. 2008; 3:e1468. [PubMed: 18213377]
29. Pomerening JR, Sontag ED, Ferrell JJ. Nat Cell Biol. 2003; 5:346–351. [PubMed: 12629549]
30. Murray AW, Kirschner MW. Science. 1989; 246:614–621. [PubMed: 2683077]
31. Orlando DA, Lin CY, Bernard A, Wang JY, Socolar JE, Iversen ES, Hartemink AJ, Haase SB. Nature. 2008; 453:944–947. [PubMed: 18463633]
32. Lu Y, Cross FR. Cell. 2010; 141:268–279. [PubMed: 20403323]

### Insight, innovation, integration

With a simple but robust microfluidic device, we characterized the cell cycle response to periodic nutrient modulation. We observed that the nutrient signal of particular period can generate resonance in cell cycle control systems so that the colony is synchronized. It is the first time that the course of synchronizing wild-type colonies in the nutrient environment was traced at single cell resolution, which demonstrated how and to what extent the cell division and growth are coupled. A stochastic model was constructed to account for our observations and to predict the efficiency of modulation schemes. Our work may shed light on the coupling between the cell division and metabolic system as well as provide a nontoxic and non-invasive method to continuously synchronize the cell cycle.

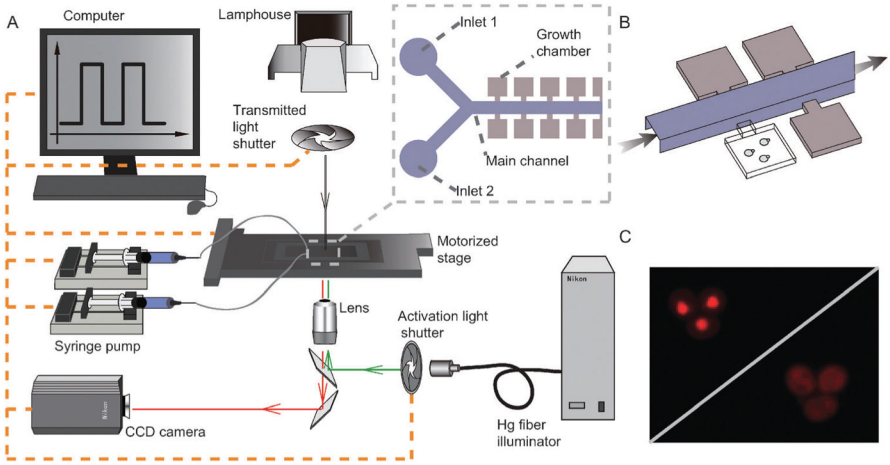


**Fig. 1.**

Microfluidic device used in this study. (A) The microfluidic cell culture chip was fixed on the motorized stage of an inverted microscope, which makes the multipoint data acquisition possible. Two kinds of culture media were perfused alternately with the help of two syringe pumps. Transmitted light from a halogen lamp house and activation light from a fiber illuminator were controlled by two shutters, respectively, so the CCD camera can acquire both bright field and fluorescent images. The cell culture and data acquisition course were controlled by computer programs. Inset, layout of our microfluidic chip. (B) The 3D structure of part of our microfluidic chip. Culture medium was fed through a higher (more than 10 μm) main channel, cell colonies were constrained in the lower (about 3.5 μm) chambers that distributed alongside of the main channel, medium and metabolites exchange between the channel and the chambers is achieved through the fine necks connecting them. (C) Top left: micrograph of the $G_1$ phase cells in which the MCM marker is localized in the nucleus (bright red dots); bottom right: non-$G_1$ phase cells in which the MCM marker is diffused throughout the cytoplasm.

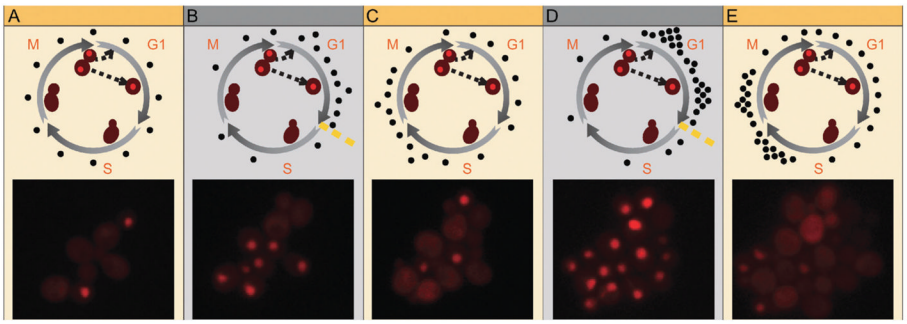


**Fig. 2.**

Cell population synchronization mechanism. (A) In untreated yeast population, cells distributed throughout the cell cycle phase, no significant accumulation in any phases is apparent. (B) During the first starvation period, cells tend to be blocked and thus accumulate in the $G_1$ phase. (C) When rich medium is supplied, cells progress out of the $G_1$ phase. (D) When the population progresses to the entrance of the next $G_1$ phase, the second nutrient limiting wave is applied, elevating the degree of synchronization. (E) When the block is retracted by flowing in rich medium, the $G_1$ index drops again. Upper panel: schematic illustration; lower panel: images of a yeast population.

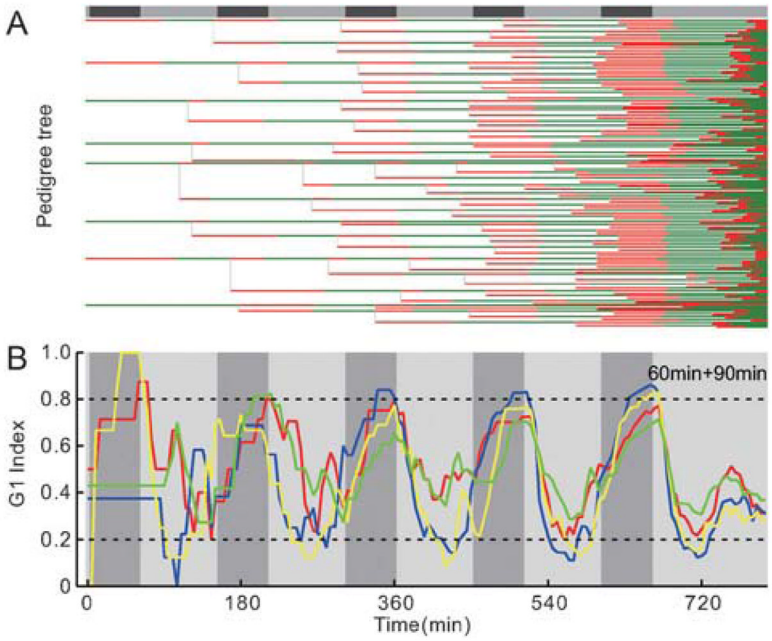


**Fig. 3.**

Pedigree tree and $G_1$ index of colonies synchronized with the repeated modulation of 60 min poor medium followed by 90 min rich medium. (A) Horizontal bar at the top of the figure indicates nutrient conditions. Nutrient depletions (black sections) are repeated 5 times, separated by adequate nutrient supplies (grey sections). Each line represents a cell. $G_1$ and non-$G_1$ phases are indicated with red and green colors, respectively. There are 8 cells (who are offsprings of one single cell which was loaded into the microfluidic chip before modulation) in this colony at the beginning of the modulation, and more than 200 cells at the end. (B) $G_1$ indices of four different colonies modulated with the same scheme (60 min poor + 90 min rich), as indicated with different colors. Dark and light grey background areas show the poor and rich medium periods, respectively.

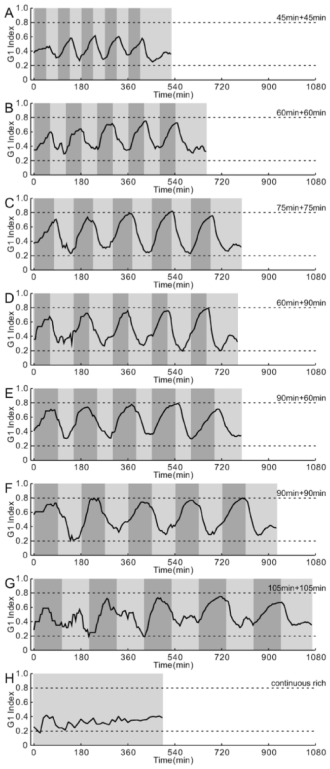


**Fig. 4.**

The $G_1$ index under different nutrient modulation schemes. For each modulation scheme, the $G_1$ index is averaged over several colonies to ensure a total of over 800 cells at the end of each experiment. Dark grey areas indicate poor medium periods and light grey areas rich medium. (A) 45 min poor medium (p) + 45 min rich medium (r). (B) 60 min p + 60 min r. (C) 75 min p + 75 min r. (D) 60 min p + 90 min r. (E) 90 min p + 60 min r. (F) 90 min p + 90 min r. (G) 105 min p + 105 min r.

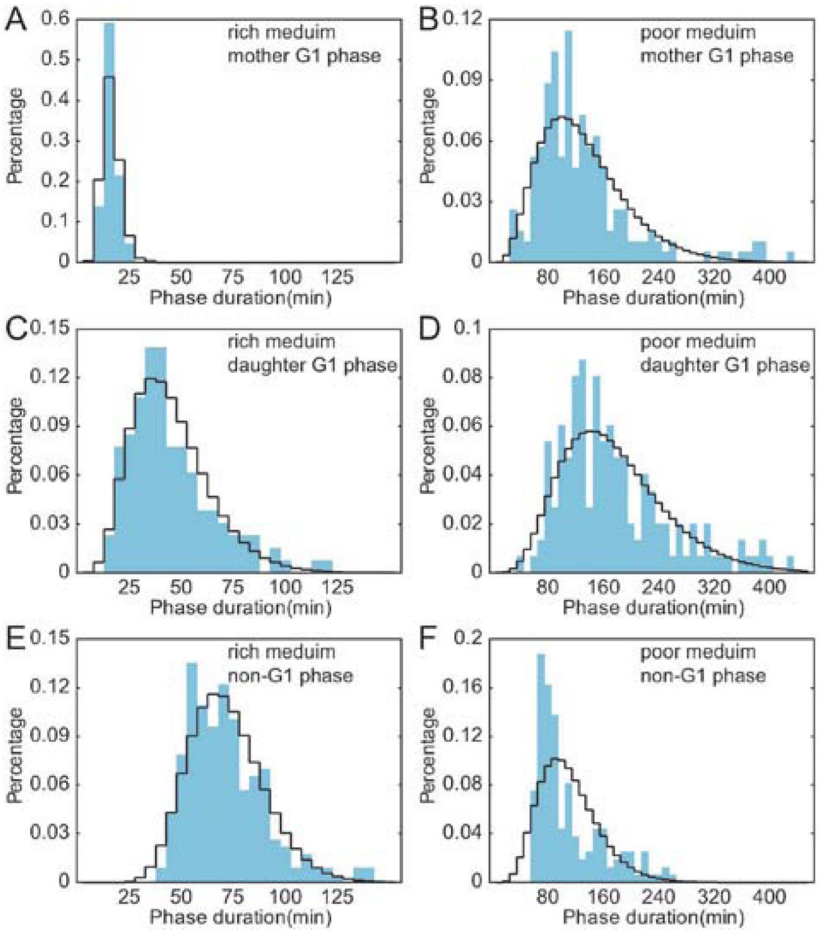


**Fig. 5.**

The duration distribution of cell cycle phases. Blue pillars correspond to the experimental measurements, black profiles indicate the fitting to a negative binomial distribution. (A) The $G_1$ phase of mother cells in rich medium (130 samples). (B) The $G_1$ phase of mother cells in poor medium (192 samples). (C) The $G_1$ phase of daughter cells in rich medium (130 samples). (D) The $G_1$ phase of daughter cells in poor medium (149 samples). (E) The non-$G_1$ phase of mother/daughter cells in rich medium (229 samples). (F) The non-$G_1$ phase of daughter/mother cells in poor medium (160 samples).

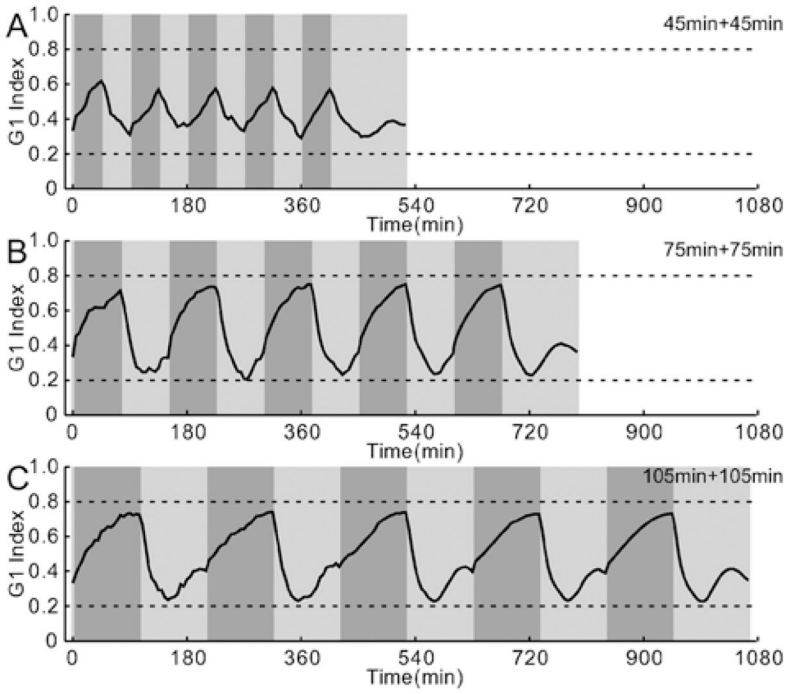


**Fig. 6.**

Simulation results of the $G_1$ index with different modulation schemes. Dark grey areas indicate poor medium stages and light grey areas rich medium. (A) 45 min poor medium (p) + 45 min rich medium (r). (B) 75 min p + 75 min r. (C) 105 min p + 105 min r.